Uncertainties in estimating B_c hadronic production and comparisons of the production at TEVATRON and LHC

Chao-Hsi Chang[1,2,a], Xing-Gang Wu[2,3,b]

[1] CCAST (World Laboratory), P.O. Box 8730, Beijing 100080, China[c]
[2] Institute of Theoretical Physics, Chinese Academy of Sciences, P.O. Box 2735, Beijing 100080, China
[3] Institute of High Energy Physics, P.O. Box 918(4), Beijing 100039, China

Abstract. The uncertainties in estimating the hadronic production of the B_c meson are studied in the framework of the complete α_s^4 approach of perturbative QCD and the gluon–gluon fusion mechanism. Quantitative comparisons of the production at TEVATRON and LHC are made. Considering the detectors at TEVATRON and LHC, we have also estimated the production with proper kinematic cuts. Based on the results, we conclude that the experimental studies of the B_c meson at the two colliders will be complementary and mutually stimulative. We find that as the CM energy is increasing from RUN-I to RUN-II at TEVATRON, the production cross section increases by about 20%.

PACS: 12.38.Bx, 13.85.Ni, 14.40.Nd, 14.40.Lb

1 Introduction

B_c-physics is attracting wide and growing interest due to experimental [1–3] and theoretical progress [4–22] (especially the experimental discovery [3]). Since the production cross section is relatively small in comparison with the production of the other heavy mesons (B, D etc.) and heavy quarkonia (J/ψ, Υ etc.), only at high energy hadronic colliders with high luminosity can one collect enough B_c events for experimental studies [4–11]. Considering the potential applications to the experimental feasibility studies on the topic, a computer program for hadronically generating the B_c meson, BCVEGPY, has been completed in [23], which has been written in Fortran and can be conveniently implemented into PYTHIA [24].

The hadronic production of the B_c-states with different spin has been estimated by a lot of authors, and all are mainly based on the gluon–gluon fusion mechanism, i.e. taking the hard subprocess $gg \to B_c + b + \bar{c}$ as the dominant one. The authors of [9,12] gave the estimate in terms of the "fragmentation approach", and the authors of [8,10,11] did it in the so-called "complete approach". The results of the two approaches agree essentially within theoretical uncertainties, especially, at high B_c transverse momentum P_T [10] and when the fragmentation approach additionally takes into account the contributions from gluon fragmentation [12]. The fragmentation approach is appropriate if one

is only interested in the information of the produced B_c itself, and its accuracy is improving with increasing P_T [10]. Comparatively, the advantage of the complete approach is that it can also retain the information of the accompanied $\bar{c}$ and b quarks (jets). For experiments, to retain more information of the events is more relevant. Therefore, in BCVEGPY [23], the complete calculation approach has been adopted.

Moreover, according to perturbative QCD (pQCD), in addition to the gluon–gluon fusion mechanism, there are several different mechanisms for the production, such as the one via the quark–antiquark annihilation subprocess $q\bar{q} \to B_c + b + \bar{c}$, and the one via the color octet mechanism etc. In [8], it is shown that the contributions to the production from quark–antiquark annihilation are much smaller than those from gluon–gluon fusion. This is mainly because of the fact that the relevant luminosity for gluon–gluon fusion is a product of the parton distribution functions (PDFs) for gluon components in the colliding hadrons, whereas that for quark–antiquark annihilation is a product of the quark and antiquark distribution functions respectively, while in a high energy collider, such as TEVATRON ($p\bar{p}$ collisions, $\sqrt{S} = 2\,\text{TeV}$) at Fermilab and LHC (pp collisions, $\sqrt{S} = 14\,\text{TeV}$) at CERN, the luminosity for gluon–gluon fusion due to parton distribution functions (PDFs) at the most kinematic region is much higher than that for quark–antiquark annihilation [27]. Furthermore, in the annihilation subprocess, there is an additional S-channel suppression from the virtual gluon propagator, which will also make contributions to the production cross section small. In the Sect. 2.3 we will make a

[a] e-mail: zhangzx@itp.ac.cn
[b] e-mail: wuxg@mail.ihep.ac.cn
[c] No correspondence address

brief comparison between those two mechanisms. According to non-relativistic QCD (NRQCD) [25], for a double heavy meson, such as $J/\psi, \eta_c, B_c, \ldots$, there may be additional color octet components which may substantially contribute to the production. The magnitude of the color octet components may be estimated with the NRQCD velocity scaling rule ($v \simeq \alpha_s(m_{B_c}) \sim 0.1$). One may find that there is no enhancement in the hadronic production (in contrast to the hidden flavored double heavy objects such as $J/\psi, \psi'$ the production which can gain one order or more in α_s via the color octet components) and the color octet components in B_c are definitely smaller than the color singlet ones (with the same input parameters, the total contributions to the hadronic production are $\lesssim v \sim v^2$ of the color singlet one); therefore, the contributions from color octet components of B_c are ignorable at leading order.

The contributions to the production from the color octet and those from the quark–antiquark annihilation mechanism were neglected in [9–13]. In BCVEGPY [23], and thus in the present paper, the mechanisms via color octet for the B_c production are ignored.

Although the estimated values for the hadronic production of B_c in the literature [9–12] are consistent within the theoretical uncertainties, in a few cases the differences on the production can reach up to almost one order of magnitude. Moreover, RUN-II of TEVATRON is taking data, LHC is under construction, and various experimental feasibility studies of B_c are in progress; thus we think to know the theoretical uncertainties quantitatively in estimates of the B_c production, and in addition, the precise comparisons of the production at LHC and TEVATRON are interesting.

The newly developed generator BCVEGPY has been well tested by carefully comparing the results with those in earlier references [8]. It, having been implemented into PYTHIA, can be conveniently applied to simulate B_c events (Monte Carlo simulation). In this paper, we highlight the uncertainties of the dominant gluon–gluon fusion mechanism, make a brief comparison of the gluon–gluon fusion mechanism and the quark–antiquark annihilation mechanism but precise comparisons of the production at TEVATRON and LHC. Although insight in certain uncertainties will enable us to understand (control) better when the next to leading order (NLO) pQCD calculation is achieved, considering that the NLO calculation cannot be available soon due to its complexity we restrict ourselves here an examination of the uncertainties only "up to" the lowest order. The uncertainties that we will examine in this paper include the variations about the running α_s, the choices of the factorization energy scale, the various versions of parton distribution functions (PDFs), the values of the bound state parameters etc. To be useful references, the production with possible kinematic cuts, which roughly "match" the detectors at TEVATRON and at LHC, is also investigated.

It is known that at high energy hadronic colliders, numerous B_c events may be produced; moreover, due to the fact that the B_c meson has a quite large branching ratio to decay into a B_s meson (several tens percent) [16–18];

thus, in principle, copious and precisely tagged B_s mesons at the production position may be collected through the inclusive decays of B_c at the hadronic colliders (B_c ($\bar{B}_c$) is the charged meson; as long as the charge of B_c ($\bar{B}_c$) and/or its decay products is determined, the produced B_s ($\bar{B}_s$) mesons through the decays of B_c ($\bar{B}_c$) are tagged precisely at the decay vertex of B_c ($\bar{B}_c$)). Studying B_s–$\bar{B}_s$ mixing and CP violation are very interesting topics and can be done only in a hadronic environment. For experimental studies of B_s–$\bar{B}_S$ mixing and a certain CP violation in B_s decays, the B_s mesons being tagged at their production position are crucial. In a hadronic environment to obtain copious B_s mesons which are precisely tagged at their production positions, the way through B_c decays is worth for considering seriously, especially at LHC. In addition, potentially this way has a great advantage in rejecting backgrounds and deducing the systematic errors [5]. Therefore the feasibility for studying the B_s mesons in this way should be investigated carefully, especially, by means of Monte Carlo simulating the events under specific detector environment so as to see the precise efficiency to have the tagged $B_s(\bar{B}_s)$ mesons and whether the idea is really practicable or not.

This paper is organized: following the Introduction, in Sect. 2 we present the studies of the uncertainties in the estimates of the hadronic production for the dominant mechanism of gluon–gluon fusion and also a brief comparison between the mechanisms of gluon–gluon fusion and quark–antiquark annihilation. In Sect. 3, we present the production with possible kinematic cuts, which roughly matches the detector situation at TEVATRON and LHC. We also compute the production at TEVATRON with CM energy changes from RUN-I to RUN-II. In the last section, we present some discussion and a short summary.

2 The uncertainties in estimates

As stated in the introduction, there are two mechanisms for the lowest order of pQCD α_s^4 approach in the hadronic B_c production, the gluon–gluon fusion and the quark–antiquark annihilation. Of them the gluon–gluon fusion mechanism is the dominant one, and there are 36 Feynman diagrams for its subprocess. The typical Feynman diagrams for the subprocess are plotted in Fig. 1a. In comparison, for the other mechanism, its subprocess is of quark–antiquark annihilation and there are 7 Feynman diagrams. The typical ones are plotted in Fig. 1b. In fact, if we consider the production only through the dominant gluon–gluon fusion mechanism, then the contributions from the quark–antiquark annihilation mechanism will be considered as one kind of uncertainties. In this section, firstly we will focus on the gluon–gluon fusion mechanism and then we will make a brief comparison between these two mechanisms.

To be more useful experimentally, we study the uncertainties of B_c hadronic production by means of the "complete approach", i.e., at collision CM energy $\sqrt{S}$,

$$d\sigma(S, p_T, \ldots)$$
$$= \sum_{ij} \int dx_1 \int dx_2 F_{H_1, P_1}^i \left(x_1, \mu_F^2\right) \cdot F_{H_2, P_2}^j \left(x_2, \mu_F^2\right)$$
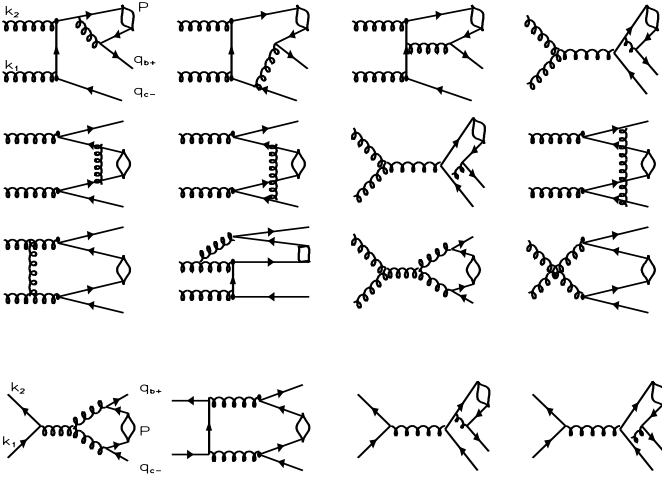
Fig. 1. a The typical Feynman diagrams for the gluon–gluon fusion subprocess; **b** The typical Feynman diagrams for the quark–antiquark annihilation subprocess

$$\cdot \, \mathrm{d}\hat{\sigma}_{ij \to B_c b \bar{c}} \left(P_1, P_2, x_1, x_2, \mu_{\mathrm{F}}^2, \hat{s}, p_{\mathrm{T}}, \dots \right) \,, \qquad (1)$$

where $F_{H_1,P_1}^i(x_1, \mu_{\mathrm{F}}^2)$ and $F_{H_2,P_2}^j(x_2, \mu_{\mathrm{F}}^2)$ are the PDFs of the incoming hadrons H_1 (momentum P_1) and H_2 (momentum P_2) for parton i (with the momentum fraction x_1) and parton j (with the momentum fraction x_2) respectively; μ_{F} is the energy scale where the factorization and renormalization for the PDFs and the hard subprocess are made; $\mathrm{d}\hat{\sigma}_{ij \to B_c b \bar{c}}$ is the differential cross section of the relevant hard subprocess, in which $\hat{s} = x_1 x_2 S$ is the CMS energy of the subprocess and p_{T} is the transverse momentum of B_c. In the subsections below, we discuss the uncertainties which are from the non-perturbative factors and from those related to the hard subprocess.

2.1 The uncertainties relevant to the parameters of potential model and masses of quarks and the meson

For all the approaches and the color singlet mechanisms of B_c production, the "decay constant" f_{B_c} relating the hadron matrix element, as one of important input parameters, is needed as input, and so far it may be calculated either by the potential model [14] or by lattice QCD [15], while in the parer, we will make discussions related to it of the potential model only. Within the potential model, it directly relates to the wave function at the origin of the binding system in terms of the following formula:

$$f_{B_c}^2 = \frac{12|\Psi_{[1S]}(0)|^2}{m_{B_c}} \,, \qquad (2)$$

where m_{B_c} is the B_c meson mass, $\Psi_{[1S]}(0)$ is the wave function at the origin of the binding system $(c\bar{b})$ at the $[1S]$ level. Since the spin splitting effects are ignored here, there is no difference for the decay constant between the spin states $[^1S_0]$ and $[^3S_1]$. There are several parameters in the potential model, which need to be fixed by fitting the experimental data of the heavy quarkonia $((c\bar{c})$ and $(b\bar{b})$,

so when computing the spectrum and the wave functions of the $(c\bar{b})$ system [14], certain uncertainties from the fitting procedure will cause some uncertainties to f_{B_c}. In the leading order (LO) approximation for the production, f_{B_c} appears in the amplitude as a linear factor exactly, so the production cross sections are proportional to it squared. Therefore, the uncertainties in the production from f_{B_c} can be figured out straightforwardly, so throughout the paper, we will fix the value $f_{B_c} = 0.48\,\mathrm{GeV}$ for the ground states (the relevant uncertainties would be figured out if need).

In addition to the decay constant f_{B_c}, the quark mass values m_c and m_b also "generate" uncertainties for the hadronic production. If all of the rest parameters in the potential might be fixed, then the values of quark masses would determine the decay constant f_{B_c}, the meson mass m_{B_c} etc. completely. However at present, the parameters in the potential model, which also appear in the formula (1), cannot be completely fixed by fitting the available data of the heavy quarkonia, so the relations of the quark masses to the decay constant f_{B_c}, the meson mass etc. cannot be well determined. Therefore, when studying the uncertainties for the hadronic production, we can consider all of the factors, explicitly appearing in the potential model and in the formula for the subprocess (1), in a "factorized" way. Furthermore, since B_c is the non-relativistic and weak-binding bound state, at LO the relative momentum between the constitute quarks can be ignored, e.g., we approximately have $m_{B_c} \simeq m_b + m_c$.

Throughout this paper, we study the uncertainties in "a factorization way", i.e., all of the parameters vary independently in their reasonable regions. For instance, when focussing on the uncertainties from m_c, we let it be a basic "input" parameter varying in the possible range

$$1.3\,\mathrm{GeV} \leq m_c \leq 1.8\,\mathrm{GeV}, \qquad (3)$$

with all the other factors, including the b quark mass, the decay constant f_{B_c} etc. being fixed.

The uncertainties from m_c are indicated by the calculated total cross sections with the m_c of (3), which are given in Table 1. Note that for the mass of B_c, the experimental result is $m_{B_c} = 6.4 \pm 0.4\,\mathrm{GeV}$ [3], while the prediction by the potential model gives $m_{B_c} = 6.1 \sim 6.3\,\mathrm{GeV}$ [14] and that by lattice QCD is about $6.4\,\mathrm{GeV}$ [15]. Thus with $m_b = 4.9\,\mathrm{GeV}$ and $m_{B_c} \simeq m_b + m_c$, the obtained m_{B_c} is in the region of theoretical prediction as well as experimental measurement. The uncertainties from m_b can be analyzed in a similar way, where the b quark mass runs over the range

$$4.5\,\mathrm{GeV} \leq m_b \leq 5.3\,\mathrm{GeV}. \qquad (4)$$

The results for various b quark masses are put in Table 2. In Tables 1 and 2, the total cross section for the hadronic production of $B_c[1^1S_0]$ and $B_c^*[1^3S_1]$ at TEVATRON and LHC are computed, where the other factors are fixed precisely as follows: the PDFs are taken as CTEQ5L [26]; the strong coupling α_{s} is in leading order and the factorization energy scale is taken to be $\mu_{\mathrm{F}}^2 = Q^2 = \hat{s}/4$, where $\hat{s}$ is the CM energy squared of the subprocess.

From the tables, one may observe how the values of m_c and m_b affect the cross section up to a sizable degree.

Table 1. The total cross section (in units nb) for hadronic production of $B_c[1^1S_0]$ ($B_c^*[1^3S_1]$) with various values of the c quark mass m_c and fixed b quark mass $m_b = 4.9$ GeV. For definiteness and focussing the uncertainties from the quark masses alone, the rest of the uncertainty sources are fixed: the mass of the meson B_c, $m_{B_c} = m_c + m_b$; the gluon distribution function is taken from CTEQ5L; the factorization energy scale is chosen $\mu_F^2 = Q^2 = \hat{s}/4$ and the running α_s is of leading order

–	TEVATRON ($\sqrt{S} = 2.$ TeV)						LHC ($\sqrt{S} = 14.$ TeV)					
m_c (GeV)	1.3	1.4	1.5	1.6	1.7	1.8	1.3	1.4	1.5	1.6	1.7	1.8
σ_{B_c} (nb)	4.84	3.87	3.12	2.56	2.12	1.76	75.6	61.0	49.8	41.4	34.7	28.9
$\sigma_{B_c^*}$ (nb)	12.3	9.53	7.39	5.92	4.77	3.87	194.	153.	121.	97.5	80.0	66.2

Table 2. The total cross section (in units of nb) for hadronic production of $B_c[1^1S_0]$ and $B_c^*[1^3S_1]$ with various values of the b quark mass m_b and fixed c quark mass $m_c = 1.5$ GeV. For definiteness and focussing the uncertainties from the quark masses alone, the gluon distribution function is taken from CTEQ5L; the factorization energy scale is chosen $\mu_F^2 = Q^2 = \hat{s}/4$ and the running α_s is of leading order

–	TEVATRON ($\sqrt{S} = 2.$ TeV)					LHC ($\sqrt{S} = 14.$ TeV)				
m_b (GeV)	4.5	4.7	4.9	5.1	5.3	4.5	4.7	4.9	5.1	5.3
σ_{B_c} (nb)	4.10	3.55	3.12	2.70	2.38	63.4	56.2	49.8	44.1	39.6
$\sigma_{B_c^*}$ (nb)	9.43	8.35	7.39	6.59	5.89	148.	133.	121.	110.	100.

Roughly speaking, both at TEVATRON and LHC, when m_b increases by steps of 0.2 GeV, then the cross section decreases by $10\% \sim 20\%$, while when m_c increases by steps of 0.1 GeV, the cross section also decreases by $10\% \sim 20\%$.

In further investigations of this paper when examining the uncertainties from the rest factors, we shall take the values $m_c = 1.5$ GeV and $m_b = 4.9$ GeV for the quark masses.

2.2 Uncertainties relevant to the QCD parameters and PDFs

In this subsection, let us focus on the gluon–gluon fusion mechanism only.

As is shown in (1), the PDFs $F^i_{H_1(P_1)}(x_1, \mu_F^2)$ and $F^j_{H_2(P_2)}(x_2, \mu_F^2)$, with $H_1 = $ proton, $H_2 = $ proton for LHC, and $H_1 = $ proton, $H_2 = $ antiproton for TEVATRON, generate uncertainties in the production. The PDFs are of a non-perturbative nature, and in (1) they have been factorized out at the energy scale μ_F with the help of pQCD factorization theorem. Usually the factorization is carried out at Q^2, a characteristic energy scale for the hard subprocess, i.e. $\mu_F^2 = Q^2$, so we use Q^2 and μ_F^2 on an equal footing throughout this paper.

As stated in the Introduction, all the estimates of the production are of leading (the lowest) order of pQCD, and then how to choose the energy scale Q^2 is a very tricky problem. If Q^2 is chosen properly, the results may be quite accurate[1]. From experience, for a hard subprocess with a two-body final state, generally when taking $Q^2 = \frac{1}{4}\hat{s}$ ($\sqrt{\hat{s}}$ is the CM energy of the subprocess), we can achieve quite an accurate result for LO calculations. However, in the present case, the gluon–gluon fusion subprocess is of a three-body final state and contains heavy quarks, so there are ambiguities in choosing Q^2, and various choices of Q^2 would generate quite different results. Since such a kind of ambiguity cannot be justified by the LO calculation itself, we take it as the uncertainty of the LO calculation, although when the NLO calculation of the subprocess is available, the uncertainty will become under control a lot more. While the NLO calculation is very complicated and it cannot be available in the foreseeable future, here we take Q^2 as a possible characteristic momentum of the hard subprocess being squared. Having reviewed the choices of Q^2 in the literature, in the following we choose a few typical examples to study this kind of uncertainties.

According to the factorization, the running of α_s and PDFs should be of leading logarithm order (LLO), and the energy scale Q^2 appearing in the calculation should be taken as one of the possible characteristic energy scales of the hard subprocess. In principle, as has been shown in [7–13], there are several typical ways to choose the energy scale Q^2 and to relate it to a characteristic energy scale ($Q^2 \gg \Lambda_{\mathrm{QCD}}^2$) of the subprocess, such as $Q^2 = 4m_c^2$, $Q^2 = 4m_b^2$, $Q^2 = p_T^2 + m_{B_c}^2$ (the "transverse mass" squared of B_c), $Q^2 = \frac{1}{4}\hat{s}$ etc. When

---

[1] In PYTHIA the value of Q^2 can be definitely fixed at each interaction vertex; therefore, when applying PYTHIA to the production, there is no energy scale ambiguity. However, in PYTHIA all kinds of b hadron ($B_s, B_c, \Lambda_b, \ldots$) events will be produced according to the proper fragmentation possibili-

ties, among which the fragmentation possibility for B_c is quite small [7,9]; thus in terms of PYTHIA to generate the B_c events is not "economical", i.e., when simulating the B_c events, enormous unwanted b hadron events with higher probability will be generated in the meantime. By contrast, the approach which we have adopted here has a quite high efficiency to generate the B_c events, though the uncertainties from the choices of Q^2 are unavoidable.

Table 3. Total cross section for the hadronic production of $B_c[1^1S_0]$ and $B_c^*[1^3S_1]$ at TEVATRON and at LHC with the leading order (LLO) running α_s and the characteristic energy scale $Q^2 = \hat{s}/4$ or $Q^2 = p_T^2 + m_{B_c}^2$. The cross section is in units of nb

	CTEQ5L	CTEQ6L	GRV98L	MRST2001L	CTEQ5L	CTEQ6L	GRV98L	MRST2001L
–		$Q^2 = \hat{s}/4$				$Q^2 = p_T^2 + m_{B_c}^2$		
–				TEVATRON				
$\sigma_{B_c(1^1S_0)}$	3.12	3.79	3.27	3.40	4.39	5.50	4.54	4.86
$\sigma_{B_c^*(1^3S_1)}$	7.39	9.07	7.88	8.16	10.7	13.4	11.1	11.9
–				LHC				
$\sigma_{B_c(1^1S_0)}$	49.8	53.1	53.9	47.5	65.3	71.1	70.0	61.4
$\sigma_{B_c^*(1^3S_1)}$	121.	130.	131.	116.	164.	177.	172.	153.

studying the uncertainties on the various choices of Q^2, we precisely choose the following four types of Q^2:

Type A: $Q^2 = \hat{s}/4$, the CM energy squared of the subprocess that is divided by 4;
Type B: $Q^2 = p_T^2 + m_{B_c}^2$, the transverse mass squared of the B_c meson;
Type C: $Q^2 = \hat{s}$, the CM energy squared of the subprocess;
Type D, $Q^2 = p_{Tb}^2 + m_b^2$, the transverse mass squared of the b quark.

Since the PDFs can be obtained only through global fitting of the experimental data and evolving them to the requested characteristic scale Q^2 in the standard way of pQCD, so there are several groups, CTEQ [26,27], GRV [28] and MRS [29] etc., who devote themselves to offer accurate PDFs to the world and to keep PDFs updated as soon as possible when new relevant experimental data are available. Thus in the literature, different versions of PDFs (including different issues by the same group) are used in the estimates of the hadronic production. To study the uncertainties due to various versions of PDFs, we consider the above mentioned three groups.

The generator BCVEGPY is programmed based on the dominant subprocess to LO pQCD only, to be self-consistent, when applying BCVEGPY we shall adopt the LO PDF. Thus we take CTEQ6L [27], CTEQ5L [26], GRV98L [28] and MRST2001L [29] as typical examples for PDFs. The versions of the gluon distributions ended with "L" are accurate up to the leading logarithm order (LLO), i.e., their QCD evolution effects with running α_s are included, so for the production to show the uncertainties correctly up to LO accuracy, it is necessary for the PDFs, the hard subprocess and the QCD "coupling constant" α_s "run" to the energy scale Q^2 properly. The running α_s in the PDFs and in the subprocess should be the same, and then, when computing the production and taking the PDFs from one version of the three groups, the running α_s should also be taken from the same group.

For comparison between TEVATRON and LHC and to pinpoint the uncertainties from PDFs, the running α_s and the choices of the characteristic energy scale Q^2, we calculate the production cross sections according to four types of PDFs, the strong coupling α_s up to LLO fixed by the PDFs and the characteristic Q^2 chosen as Type A and Type B. The obtained results are shown in Table 3. From the table, we can see that the gluon distribution functions, the running coupling constant and the corresponding energy scale all affect the cross section to certain degrees.

For all of the LO PDFs, the differences in the corresponding cross sections given by them are small (about 10%–20%). But the choice of Q^2 as Type A and Type B causes the cross section to change by a factor of about $\frac{1}{4}$ to $\frac{1}{3}$, which is a comparatively large effect. From Table 3, one may see that the cross section at TEVATRON and at LHC presents a somewhat different aspect of the cross section. Roughly speaking at TEVATRON CTEQ6L is the biggest, while at LHC, GRV98L is the biggest, under a certain characteristic energy scale such as Q^2 in Type A.

From Table 3, we may also see that the cross section of the B_c meson production at LHC is at least one order larger in magnitude than that at TEVATRON. This is mainly due to the fact that LHC has a much higher collider energy than TEVATRON, so the lowest boundary of the momentum fractions x_i $(i = 1, 2)$ at LHC is much smaller than that at TEVATRON, and then there are more interacting partons at LHC than at TEVATRON, i.e. gluons which have a CM energy above the threshold for the subprocess, in the collision hadrons.

When the produced B_c mesons with a small p_T are too close to the collision beam, they cannot be measured experimentally, so we calculate the cross sections with transverse-momentum cuts p_{Tcut}. For comparison, we define the following ratio of the integrated cross sections for TEVATRON and LHC: $R = \left(\frac{\sigma_{\text{TEVATRON}}}{\sigma_{\text{LHC}}} \right)_{p_{Tcut}}$ and put the results for $B_c[1^1S_0]$ in Table 4.

To show the uncertainties due to various factors more quantitatively, let us compute the differential cross sections of p_T and y for the pseudo-scalar B_c meson and draw the curves accordingly.

From Fig. 2, we may see that the differential distributions for the three PDFs CTEQ5L, GRV98L and

Table 4. Dependence of the ratio $R = \left(\frac{\sigma_{\text{TEVTRON}}}{\sigma_{\text{LHC}}} \right)$ on p_{Tcut} for $B_c[1^1S_0]$, where $Q^2 = \hat{s}/4$, the running α_s is in LO and the gluon distribution is CTEQ5L

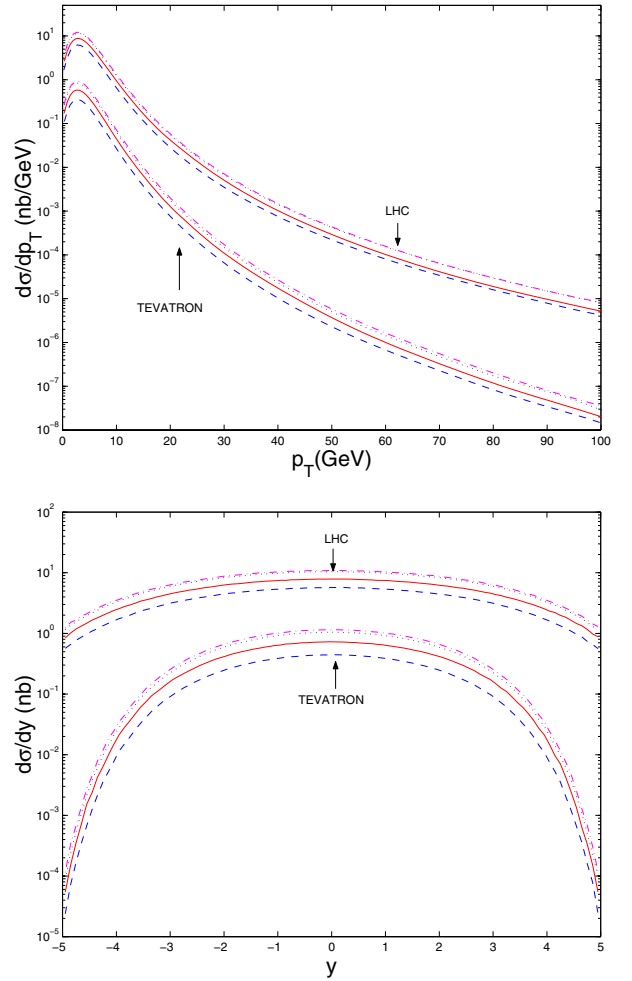| –		B_c				B_c^*		
P_{Tcut} (GeV)	0	5	50	100	0	5	50	100
R $(\times 10^{-2})$	6.26	5.24	1.00	0.31	6.09	5.19	0.97	0.24
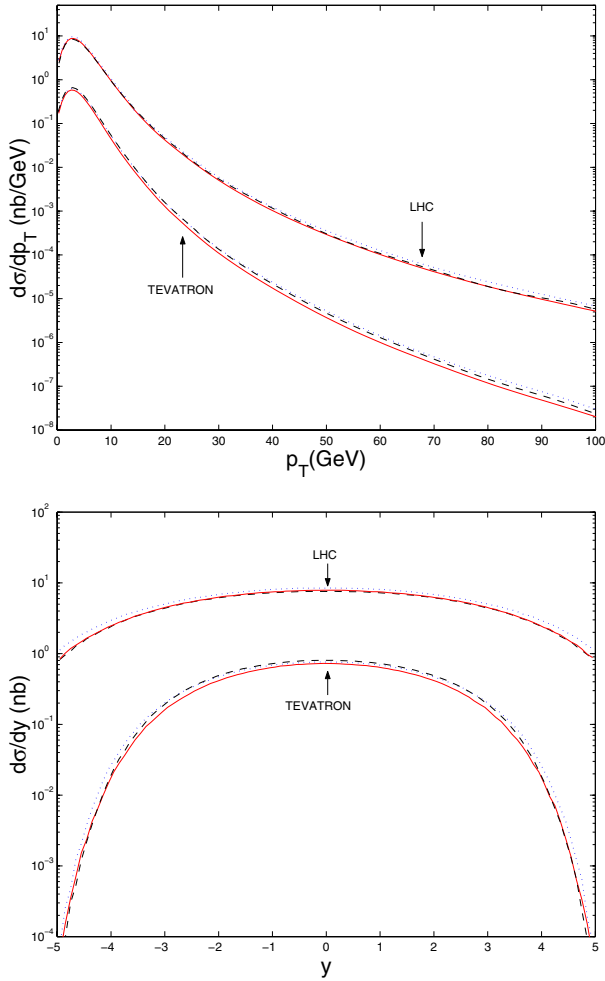
Fig. 2. B_c differential distributions versus its transverse momentum p_T and rapidity y for different versions of gluon distributions in leading order. The characteristic energy scale is taken as $Q^2 = \hat{s}/4$. Solid line: CTEQ5L; dotted line: GRV98L and dashed line: MRST2001L. The upper (lower) three lines correspond to the distributions in LHC (TEVATRON)
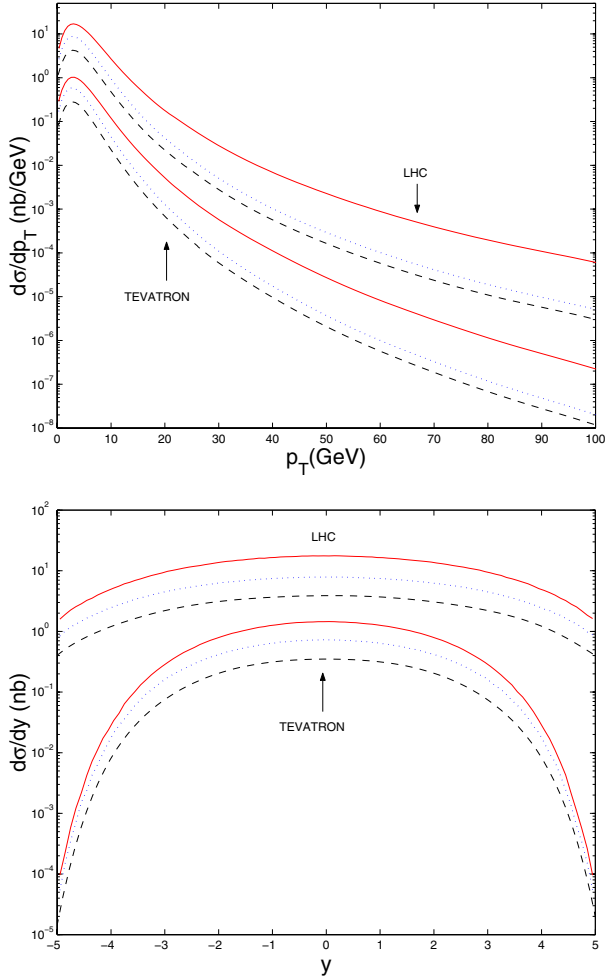

Fig. 3. B_c differential distributions versus its transverse momentum p_T and rapidity y for four typical choices of the characteristic energy scale Q^2. The gluon distribution is chosen as CTEQ5L and the running α_s is in leading order. The choice of Q^2 is solid line Type A; dotted line Type B; dashed line Type C and dash-dot line Type D. The upper (lower) four lines correspond to the distributions at LHC (TEVATRON)

MRST2001L are very similar. The corresponding differences for TEVATRON and LHC are evident (the differences as shown in Table 3 are less than 20%). In regions of comparatively small p_T and y in TEVATRON the distributions of p_T and y obtained with MSRT2001L are the largest, and then those of GRV98L and CTEQ5L; while at LHC, those of GRV98L are the largest, and then those of CTEQ5L and MSRT2001L. From the figure, we also see that the p_T distributions in TEVATRON are steeper than those in LHC.

Since in the literature, various α_s have been adopted in making estimates of the B_c production [8–13], so to follow these authors, we try several α_s to compute the production. Namely, in addition to the LO α_s, the constant $\alpha_s = 0.22$ and the NLO α_s are also taken into the computations and the curves of the production obtained by the various α_s are drawn in Fig. 4.

We may see from Fig. 4 that the variations of the results are quite large for both TEVATRON and LHC; those with

$\alpha_s = 0.22$ are the largest, those with NLO α_s are the smallest, while those with LO α_s are in the middle.

In summary, of all the uncertainties which have been studied in this subsection, the uncertainty caused by the different choice of Q^2 is the largest; it can be as great as a factor around $\frac{1}{3}$ (although in the literature results with various choices of the running α_s have given rise to even a greater change).

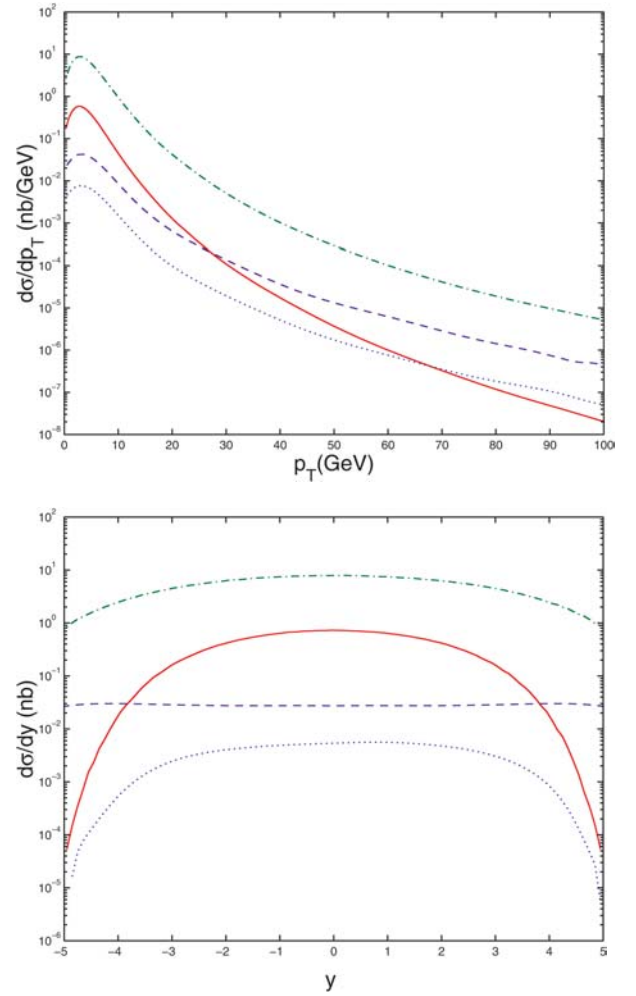## 2.3 Comparison between the mechanisms of gluon–gluon fusion and quark–antiquark annihilation

In this subsection we make a brief comparison of the mechanisms of gluon–gluon fusion and quark–antiquark annihilation. Since in a hadron such as $P, \bar{P}, \pi, \ldots$, the PDFs of heavy quarks are very small throughout the active region $|x_i| \leq 1$, it is sufficient to take into account only the light quark pair (u–$\bar{u}$, d–$\bar{d}$ and s–$\bar{s}$) annihilations.

Fig. 4. B_c differential distributions versus its transverse momentum p_T and rapidity y for different running α_s. The gluon distribution of CTEQ5L and the Type A characteristic energy scale $Q^2 = \hat{s}/4$, are used here. The solid line stands for the constant $\alpha_s = 0.22$, the dotted line for the leading order running α_s and the dashed line for the next to leading order running α_s. The upper (lower) three lines correspond to the distributions in LHC (TEVATRON)

Fig. 5. B_c distributions versus its transverse momentum p_T and rapidity y of B_c due to gluon–gluon fusion and quark–antiquark annihilation (the direction of positive y is defined as that of the momentum of the colliding proton). The PDFs are taken from CTEQ5L, the running α_s is set at leading order, and $Q^2 = \frac{1}{4}\hat{s}$. The solid lines correspond to gluon–gluon fusion and the dotted lines to quark–antiquark annihilation in TEVATRON. The dashed-dotted lines correspond to gluon–gluon fusion and the dashed lines to quark–antiquark annihilation in LHC

Now we come to the comparative results for the gluon–gluon fusion and the quark–antiquark annihilation mechanisms. In Fig. 5, we show the appropriate B_c distributions.

From Fig. 5 we see that for production at a high energy, such as TEVATRON and LHC, the gluon–gluon fusion mechanism is dominant over the quark–antiquark annihilation mechanism, typically when the transverse momentum $p_T \leq 60\,\mathrm{GeV}$ and rapidity $|y| \leq 5.0$. Only in TEVATRON do the contributions from gluon–gluon fusion become smaller than those from quark–antiquark annihilation when $p_T \geq 70\,\mathrm{GeV}$. Generally speaking, for the transverse-momentum distributions, at low p_T the contributions from gluon–gluon fusion are greater than those from quark–antiquark annihilation by at least two orders of magnitude for both LHC and TEVATRON. For high transverse momentum ($p_T \geq 70\,\mathrm{GeV}$), the difference in the two mechanisms changes sign in TEVATRON (i.e. contribu-

tions from quark–antiquark annihilation become greater than those from gluon–gluon fusion due to the fact that with such a high p_T, the valence quark PDFs play a significant role), but in LHC the contributions from gluon–gluon fusion are still greater by an order of magnitude than those from quark–antiquark annihilation. For rapidity y distributions, in the $|y| \simeq 0$ region the contributions from gluon–gluon fusion are greater by two orders of magnitude in both colliders; but in TEVATRON in the higher region of $2.0 \leq |y| \leq 5.0$, contributions from the valence quarks' annihilations become more important, so that contributions from quark–antiquark annihilation increase remarkably (though still below those from gluon–gluon fusion). It is interesting to note that there is a slight asymmetry in the rapidity y of the meson B_c for the quark–antiquark annihilation subprocess. In TEVATRON concerns $P\bar{P}$ collision,

so the asymmetry in y is maintained somewhat (see Fig. 5). We will describe this feature in TEVATRON elsewhere [30].

The contributions from the quark–antiquark annihilation mechanism to B_c hadronic production, compared with those from the gluon–gluon fusion mechanism, can be ignored safely in LHC in the allowed kinematic region. In TEVATRON, they can also be ignored over most of the allowed kinematic region, i.e., only a small allowed kinematic region is an exception. In this paper, therefore, we consider the gluon–gluon fusion mechanism mainly.

3 Kinematic cuts for the hadronic production of the B_c meson

Experimentally, there is no detector which can cover all the kinematics of the events, so only some of the B_c producing events can be observed completely. For instance, in a high energy hadronic collider, the B_c events with a small p_T and/or a large rapidity y (the produced B_c mesons move very close to the beam direction) cannot be detected by the detectors directly, so this kind of events cannot be utilized for experimental studies in common cases. Therefore, only "detectable" events should be taken into account in the estimates for a specific purpose, i.e., events with proper kinematic cuts on p_T and y must precisely be put in the estimates. Considering the detectors' abilities and in order to offer experimental references, we try various cuts accordingly in the estimate of the B_c production.

First, we study the distributions of p_T and $\sqrt{\hat{s}}$ for the B_c meson with various rapidity cuts y_{cut} (here we mean that only the B_c events with $|y| \leq y_{\text{cut}}$ are taken into account), and as an example only the pseudo-scalar B_c meson is taken into account. Note that the momenta and energies of the b, $\bar{c}$ and B_c meson are measurable experimentally (a complete measurement of the events), hence the CM energy $\sqrt{\hat{s}}$ of the subprocess is measurable, i.e., in fact the distribution of $\sqrt{\hat{s}}$ is measurable experimentally. Taking into account the abilities in measuring the rapidity of B_c for the detectors CDF, D0 and BTeV at TEVATRON, and ATLAS, CMS and LHC-B at LHC, various possible rapidity cuts, $y_{\text{cut}} \sim 1.5$ or higher, are tried. To project out the cut effects, here we fix for use the CTEQ5L as gluon distribution function, LO running α_s and Type A energy scale ($Q^2 = \hat{s}^2/4$) to carry out the study. The results for the distributions of p_T and $\hat{s}$ with various y-cuts are shown to have a similar behavior; thus we do not plot the curve here but note that the dependence of the differential distributions on y_{cut} and p_{Tcut} for LHC is stronger than that for TEVATRON. This is because at TEVATRON, all the distributions with sizable rapidity cover a smaller region in y. The correlations between p_T and y are interesting, so we plot the y distributions with various p_T-cuts over a wide range of $p_{\text{Tcut}} : 5.0 \sim 100\,\text{GeV}$, in Fig. 6. From this figure, the dependence of the differential distributions on rapidity y with different p_{Tcut} at LHC exhibits a broader profile than that at TEVATRON.

The p_T distributions of the production vary with y_{cut} mainly due to the fact that as p_T increases, the dependence
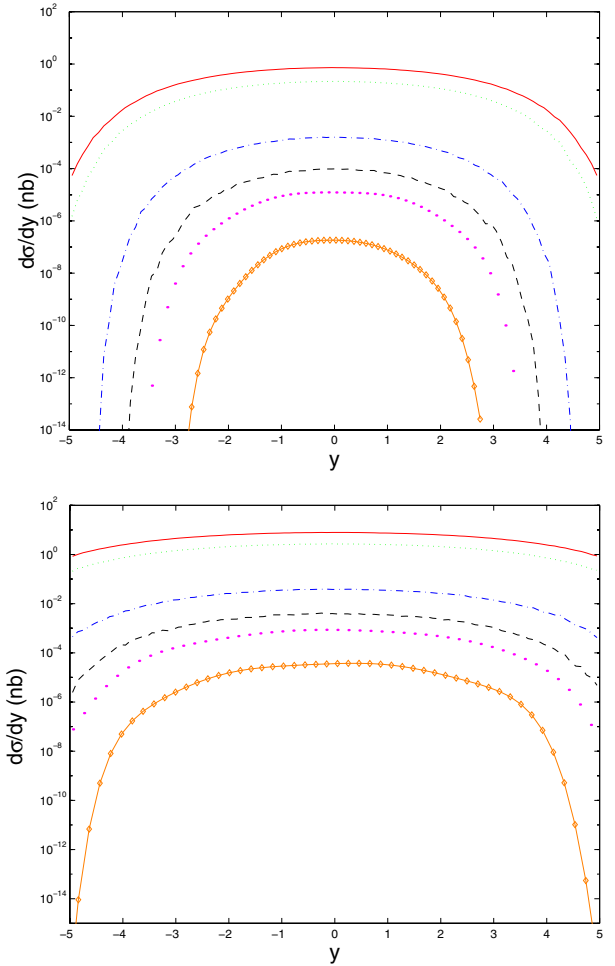
Fig. 6. B_c differential distributions versus its y with various p_{Tcut} in TEVATRON (upper diagram) and in LHC (lower diagram). A solid line corresponds to the full production without p_{Tcut}; a dotted line to $p_{\text{Tcut}} = 5.0\,\text{GeV}$; a dash-dot line to $p_{\text{Tcut}} = 20.0\,\text{GeV}$; the dashed line to $p_{\text{Tcut}} = 35.0\,\text{GeV}$; the big dotted line to $P_{\text{Tcut}} = 50.0\,\text{GeV}$ and the solid line with diamonds to $p_{\text{Tcut}} = 100\,\text{GeV}$

of the distribution on y becomes smaller as the value of y_{cut} becomes less important. When p_T increases to a sufficiently large value, the "plateau" of the differential distributions (see Fig. 6) becomes smaller than y_{cut} and the p_T differential distributions with and without y-cut coincide.

To analyze the quantitative differences of the differential distributions with regard to p_{Tcut} and y_{cut}, we introduce the ratio for the integrated hadronic cross sections:

$$R_{p_{\text{Tcut}}} = \left(\frac{\sigma_{y_{\text{cut}}}}{\sigma_0} \right)_{p_{\text{Tcut}}} , \qquad (5)$$

where $\sigma_{y_{\text{cut}}}$ and σ_0 are the hadronic cross section with and without y_{cut} respectively. The ratio $R_{p_{\text{Tcut}}}$ varies with p_{Tcut} and y_{cut}, and its values are given in Table 5.

From Table 5 we may see that, for a fixed y_{cut}, the value of $R_{p_{\text{Tcut}}}$ becomes larger with increasing p_{Tcut}. It is understandable that the differential distributions versus the rapidity y decrease with the increment of p_T, so the

Table 5. Values of the ratio $R_{p_{\text{Tcut}}}$ (see definition in text) for the hadronic production of the pseudo-scalar B_c meson in TEVATRON and LHC

p_{Tcut}	0.0 GeV			5 GeV			20 GeV			35 GeV			50 GeV		
y_{cut}	1.0	1.5	2.0	1.0	1.5	2.0	1.0	1.5	2.0	1.0	1.5	2.0	1.0	1.5	2.0
$R_{p_{\text{Tcut}}}$ (TEVATRON)	0.45	0.64	0.79	0.46	0.65	0.80	0.57	0.77	0.91	0.65	0.85	0.95	0.70	0.90	0.98
$R_{p_{\text{Tcut}}}$ (LHC)	0.31	0.46	0.59	0.32	0.47	0.60	0.38	0.54	0.69	0.42	0.60	0.74	0.45	0.64	0.79

Table 6. The integrated hadronic cross section for TEVATRON at different CM energies. The gluon distribution is chosen from CTEQ5L and the characteristic energy scale of the production is chosen as Type A, i.e. $Q^2 = \hat{s}/4$. In addition, a cut for transverse momentum p_T ($p_T < 5\,\text{GeV}$) and a cut for rapidity y ($|y| > 1.5$) have been imposed

CM energy	1.8 (TeV)	1.9 (TeV)	1.96 (TeV)	2.0 (TeV)
$B_c[^1S_0]$	0.40	0.44	0.46	0.47
$B_c^*[^3S_1]$	1.00	1.09	1.14	1.18

contributions to the hadronic cross section surviving after the cut (i.e. $|y| \leq y_{\text{cut}}$), increase with the increment of p_{Tcut}.

As for the B_c meson production, only in high energy hadronic colliders can numerous B_c mesons be produced. The cross section of B_c meson production is quite sensitive to the CM energy of the collider. Since RUN-II of TEVATRON is running now at a slightly higher energy than 1.8 TeV (of RUN-I), we take TEVATRON as an example to study the increase caused by slight changes in the CM energy. The CM energy for RUN-II is designed to be 2.0 TeV, so here we take energy values, 1.8, 1.9, 1.96 and 2.0 TeV to compute the cross sections. The obtained results for the values of the integrated cross section with suitable cuts are shown in Table 6. From Table 6, we see that when the CM energy of TEVATRON increases from 1.8 to 2.0 TeV, the cross section increases by about 20%.

4 Summary

In this paper we have presented quantitative studies on the uncertainties in estimates of the B_c meson hadronic production. The uncertainties have been examined in turn by "factorizing" their origins. The computations are based on the generator BCVEGPY [23] mainly. The investigated quantitatively uncertainties involve those due to various versions of PDFs given by various groups, the variations of the parameters relevant to the potential model, the strong coupling α_s relevant to its running and the characteristic energy scale Q^2 of the process where the QCD factorization is carried out etc. We find that the characteristic energy scale Q^2 of the process is the source which causes the greatest uncertainty for the LO QCD estimates. We have also shown the differences between LHC and TEVATRON for various observables with reasonable kinematic cuts, such as the cuts on the B_c meson transverse momentum p_{Tcut} and rapidity y_{cut}. We also point out that at TEVATRON from RUN-I to RUN-II due to the increase of the collision CM energy, the cross section of the B_c production

increases by about 20%. In view of the fact that TEVATRON is running while LHC is still under construction, based on our studies we can clearly see that experimental B_c studies at the two colliders are mutually stimulative and complementary. As for the topic of the study of B_s–$\bar{B}_s$ mixing and CP violations in B_s meson decays at high energy hadronic colliders with tagged B_s mesons produced through the B_c decays, since LHC has a much higher CM energy, the B_c-production cross section is higher than one order of magnitude at TEVATRON, and LHC has a much higher luminosity than at TEVATRON, and it seems that the particularly interesting topic above may be more accessible and fruitful at LHC than that at TEVATRON RUN-II, or even RUN-III.

References

1. DELPHI Collaboration, P. Abreu et al., Phys. Lett. B **398**, 207 (1997); ALEPH Collaboration, R. Barate et al., Phys. Lett. B **402**, 213 (1997); OPAL Collaboration, K. Ackerstaff et al., Phys. Lett. B **420**, 157 (1998)
2. CDF Collaboration, F. Abe et al., Phys. Rev. Lett. **77**, 5176 (1996)
3. CDF Collaboration, F. Abe et al., Phys. Rev. Lett. **81**, 2432 (1998); Phys. Rev. D **58**, 112004 (1998)
4. K. Anikeev et al., hep-ph/0201071
5. Chao-Hsi Chang, Proceedings of the XXXVIIth Rencontres de Moriond, Les Arcs, Savoie, France, 2002 QCD and High Energy Hadronic Interactions, p-27, hep-ph/0205112
6. C. Quigg, Proceedings of the Workshop on B Physics at Hadron Accelerators, Snowmass (CO) USA, 1993, edited by P. McBride, C.S. Mishra
7. Chao-Hsi Chang, Yu-Qi Chen, Phys. Rev. D **46**, 3854 (1992); Erratum D **50**, 6013 (1994)
8. Chao-Hsi Chang, Yu-Qi Chen, Phys. Rev. D **48**, 4086 (1993)
9. E. Braaten, K. Cheung, T.C. Yuan, Phys. Rev. D **48**, 4230 (1993); **48**, R5049 (1993)
10. Chao-Hsi Chang, Yu-Qi Chen, Guo-Ping Han, Hung-Tao Jiang, Phys. Lett. B **364**, 78 (1995); Chao-Hsi Chang, Yu-Qi Chen, R.J. Oakes, Phys. Rev. D **54**, 4344 (1996); K. Kolodziej, A. Leike, R. Rückl, Phys. Lett. B **355**, 337 (1995)
11. A.V. Berezhnoy, V.V. Kiselev, A.K. Likhoded, Z. Phys. A **356**, 79 (1996); S.P. Baranov, Phys. Rev. D **56**, 3046 (1997)

12. K. Cheung, Phys. Lett. B **472**, 408 (2000)
13. A.V. Berezhnoy, V.V. Kiselev, A.K. Likhoded, A.I. Onishchenko, Phys. Atom. Nucl. **60**, 1729 (1997); hep-ph/9703341
14. Yu-Qi Chen, Yu-Ping Kuang, Phys. Rev. D **46**, 1165 (1992); E. Eichten, C. Quigg, Phys. Rev. D **49**, 5845 (1994); D **52**, 1726 (1995); S.S. Gershtein, V.V. Kiselev, A.K. Likhoded, A.V. Tkabladze, Phys. Rev. D **51**, 3613 (1995)
15. C.T.H. Davies et al., Phys. Lett. B **382**, 131 (1996)
16. Chao-Hsi Chang, Yu-Qi Chen, Phys. Rev. D **49**, 3399 (1994); Commun. Theor. Phys. **23**, 451 (1995)
17. A. Abd El-Hady, J.H. Munoz, J.P. Vary, Phys. Rev. D **62**, 014014 (2000)
18. N. Isgur, D. Scora, B. Grinstein, M. Wise, Phys. Rev. D **39**, 799 (1989); M. Lusignoli, M. Masetti, Z. Phys. C **51**, 549 (1991); D. Scora, N. Isgur, Phys. Rev. D **52**, 2783 (1995); Dongsheng Du, G.-R. Lu, Y.-D. Yang, Phys. Lett. B **387**, 187 (1996); Dongsheng Du et al., Phys. Lett. B **414**, 130 (1997); Jia-Fu Liu, Kuang-Ta Chao, Phys. Rev. D **56**, 4133 (1997); P. Colangelo, F.De Fazio, Phys. Rev. D **61**, 034012 (2000); V.V. Kiselev, A.E. Kovalsky, A.K. Likhoded, Nucl. Phys. B **585**, 353 (2000); V.V. Kiselev, A.K. Likhoded, A.I. Onishchenko, Nucl. Phys. B **569**, 473 (2000); M.A. Nobes, R.M. Woloshyn, J. Phys. G **26**, 1079 (2001)
19. M.A. Ivanov, J.G. Körner, O.N. Pakhomova, Phys. Lett. B **555**, 189 (2003); A. Faessler et al., Eur. Phys. J. direct C **4**, 18 (2002); M.A. Ivanov, J.G. Körner, P. Santorelli, Phys. Rev. D **63**, 074010 (2001)
20. Chao-Hsi Chang, Shao-Long Chen, Tai-Fu Feng, Xue-Qian Li, Phys. Rev. D **64**, 014003 (2001); Commun. Theor. Phys. **35**, 51 (2001)
21. M. Beneke, G. Buchalla, Phys. Rev. D **53**, 4991 (1996)
22. Chao-Hsi Chang, J.-P. Cheng, C.-D. Lü, Phys. Lett. B **425**, 166 (1998); P. Colangelo, F. De Fazio, Mod. Phys. Lett. A **14**, 2303 (1999); Chao-Hsi Chang, Cai-Dian Lü, Guo-Li Wang, Hong-Shi Zong, Phys. Rev. D **60**, 114013, 1999; Chao-Hsi Chang, Yu-Qi Chen, Guo-Li Wang, Hong-Shi Zong, Phys. Rev. D **65**, 014017 (2001); Commun. Theor. Phys. **35**, 395 (2001); Chao-Hsi Chang, Anjan K. Giri, Rukmani Mohanta, Guo-Li Wang, J. Phys. G **28**, 1403 (2002); hep-ph/0204279; Xing-Gang Wu, Chao-Hsi Chang, Yu-Qi Chen, Zheng-Yun Fang, Phys. Rev. D **67**, 094001 (2003); hep-ph/0209125
23. Chao-Hsi Chang, Chafik Driouich, Paula Eerola, Xing-Gang Wu, Comput. Phys. Commun. **159**, 192 (2004); hep-ph/0309120
24. T. Sjostrand, Comput. Phys. Commun. **82**, 74 (1994)
25. Geoffrey T. Bodwin, Eric Braaten, G. Peter Lepage, Phys. Rev. D **51**, 1125 (1995); Erratum D **55**, 5853 (1997)
26. H.L. Lai et al., Eur. Phys. J. C **12**, 375 (2000)
27. H.L. Lai et al., hep-ph/0201195
28. M. Glueck, E. Reya, A. Vogt, Eur. Phys. J. C **5**, 461 (1998)
29. A.D. Martin, R.G. Roberts, W.J. Stirling, R.S. Thorne, Eur. Phys. J. C **23**, 73 (2002)
30. Chao-Hsi Chang, Xing-Gang Wu, The mechanism of quark–antiquark annihilation in hadronic production of the meson B_c, in preparation